Coupling of Two Rectangular Waveguides through a Diaphragm with a Dielectric Slab in the Slot

Ludmila P. Yatsuk*, **Anatoly F. Lyakhovsky,**
Victor A. Katrich, and Andrey A. Lyakhovsky

Abstract—A scattering problem for two semi-infinite rectangular waveguides coupling through a narrow slot cut in the common end wall of the two waveguides is solved. The slot is partially filled with a dissipative or perfect dielectric insert. A mathematical model based on continuity of tangential components of magnetic field vectors on both surfaces of the diaphragm in the coupling waveguides is proposed. The magnetic field in the slot is represented by a set of slot eigenwaves. The electrical field distribution function is used as a basis function in the Galerkin's procedure allowing to find unknown amplitude coefficients. Simulation and experimental measurement have been carried out. Dependences of scattering parameters upon the wavelength were studied for various geometric parameters, insert position in the slot, and insert material permittivity and losses. A good agreement between simulation results and experimental data is obtained. It was shown that an estimate of the insert permittivity and losses can be done for unknown materials using experimental and simulated data.

1. INTRODUCTION

Narrow slots in waveguide walls are widely used as antenna radiators or coupling elements between adjacent electrodynamic volumes of microwave devices with specified electrodynamic characteristics. Resonant slots are of great interest, since they effectively radiate, do not shift the phase of a wave transmitted through the slot, and can be used for creating radiation patterns of a special form. Many interesting applications can be developed using slots partially filled with dielectric. A slot can be resonantly tuned by varying its length. The tuning can be accomplished using the theory developed for dipole and slot antennas in works of prominent scientists such as Pocklington [1], Hallen [2], Leontovich and Levin [3], Watson [4], Feld [5], Stevenson [6], and others. The main problem of the theory consists in formulating functional equations for electric or magnetic currents along a wire or slot, based on boundary conditions. For the slots, continuity conditions of tangential components of magnetic field vectors should be fulfilled on the common surfaces of adjacent electrodynamic volumes. When dyadic Green's functions for these volumes are known, the functional equations can be reduced to integral or integral-differential equations of the Hallen or Pocklington type, which are equations of the first kind with singular kernels. These equations cannot be rigorously solved. Thus, the problem is reduced to solution of these equations, and the question of existence and uniqueness of solutions arises. For thin wires and narrow slots, these equations can be reduced to one-dimensional equations. The kernel of the Hallen-type equation has the logarithmic singularity, and such an equation has a unique solution [7]. Regularization of the singular integrals equations can also be carried out using the semi-inversion technique [8, 9].

The kernel singularity of the Pocklington equation is of high order. The semi-inversion method was developed for regularization of this equation in [10, 11], where the operator of the problem is represented by a sum of singular and regular operators. The eigenfunctions of the singular operator were used as basis functions in the Galerkin method. Thus, the first kind equation was transformed into a system of linear algebraic equations (SLAE) of the second kind having very good convergence. A comprehensive list of references on modern methods of problem solutions for coupling electrodynamic volumes can be found in [12, 13]. In particular, in [12] it is emphasized that different approaches to the rigorous solution of electrodynamic problems can be formally divided into two classes: 1) direct numerical and 2) numerical and analytical methods. The last ones combine an analytical formulation of the problem with a method of moments, mainly, Galerkin method. During a solving the problem a number of analytical transformations previously are carried out which provide a good convergence of resulting matrix equations. For example, such approach was realized in [10, 11]. We shall focus on possibilities of this approach application to our problem.

The integral equations for narrow slots are usually formulated by an approximation of an infinitely thin waveguide wall. The actual thickness of the waveguide wall can be taken into account by introducing an equivalent slot width [14]. But this concept cannot be applied if the slot is partially filled with dielectric.

The waveguide wall thickness can be taken into account correctly if coupling between three electrodynamic volumes is taken into account: an inner waveguide portion, where the incident wave exists, a cavity of the slot, and an external waveguide portion into which the electromagnetic field penetrates through the slot [15]. The continuity conditions for tangential components of a magnetic field on boundary surfaces of these volumes allow us to formulate functional equations for unknown electric fields. These equations may be reduced to a pair of integral equations [16] or to a system of linear algebraic equations if the problem should be solved by direct methods.

The integral equations can be solved if Green's functions for all coupled volumes are known. Since a Green's function cannot be easily built for the slot cavity with a dielectric insert, the dyadic Green's functions cannot be used for description of the electromagnetic field inside the slot. An alternative method of solving this problem was first proposed in [17, 18] and then developed in [19] for obtaining the rigorous and fast convergent solution for a rectangular waveguide coupling by a slot in the common wall.

If the problem is solved by direct methods, for example, by the Galerkin method, the solution convergence can be better if the basis functions correctly describe special features of E-field distribution in a slot. So, it is very important to choose proper functions for approximation of the E-field distribution inside the slot. A trigonometric basis, Chebyshev or Gegenbauer polynomials are often used for slots homogeneously filled with dielectric or for unfilled slots. The distribution of the slot magnetic current in the first approximation of an asymptotic method was presented in [20] as a sum of symmetric and asymmetric functions, which take into account the structure of the exciting field.

The electromagnetic field in the slot partially filled with dielectric can be represented by the eigenwave field of the slot cavity as a waveguide. This can also be done for unfilled slots. The functions describing transverse electric field of eigenwaves may be used as basis functions for electric field representation on both surfaces of the slot cut in a screen of finite thickness. Such functions were used in [21] where coupling of two rectangular waveguides through a slot cut in a common wide wall of waveguides and partially filled with dielectric was considered. In this paper we will study the properties of a narrow transverse slot partially filled with a perfect or dissipative dielectric in the diaphragm inside a rectangular waveguide.

2. THE PROBLEM STATEMENT AND SOLUTION

The system geometry is shown in Fig. 1. The waveguide is excited by the H_{10} wave incident at the diaphragm. The transverse slot is cut in the diaphragm. The slot length, width and thickness are L, d and t, respectively. The slot is partially filled by the dielectric insert. The problem solution consists in finding the diaphragm reflection and transmission coefficients, which can be found if the electric fields on the slot surfaces $S_1\,(\xi = 0)$ and $S_2\,(\xi = t)$ are known.

The electric field distribution on the surfaces S_1 and S_2 can be represented as the sum of the LE_{q0}
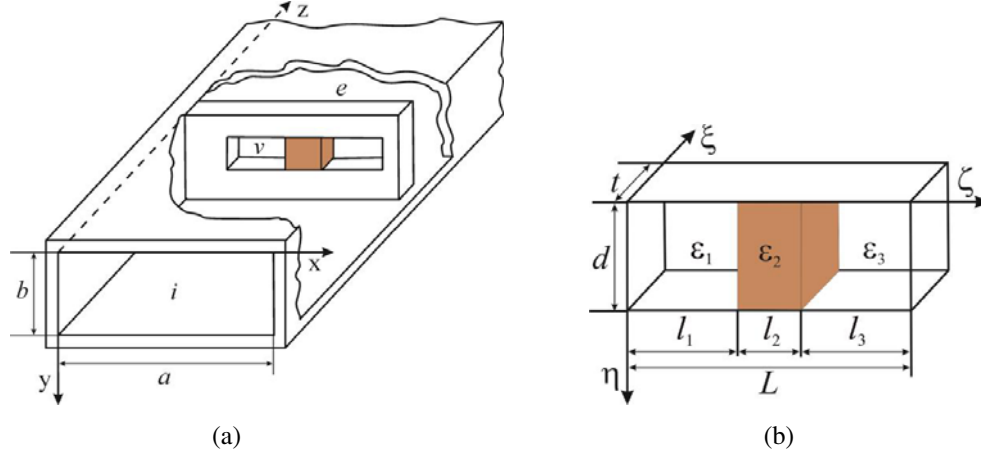
Figure 1. The system under consideration. (a) General view of the waveguide with a diaphragm. (b) Geometry of cavity of the slot.

waves in a waveguide with a three-layer dielectric. The resulting electric field $\vec{e}_{si}$ $(i = 1, 2)$ on the slot surfaces S_1 and S_2 on both sides of the diaphragm can be represented as

$$\vec{e}_{si} = \sum_{q=1}^{Q} V_{qi} \vec{e}_q, \tag{1}$$

where Q is the number of basis functions taken into account, and V_{qi} are the complex voltage amplitudes between slot edges in points of electric field maxima. The basis vector functions $\vec{e}_q$ can be written as

$$\vec{e}_q = \vec{\eta}^0 \left(1/d\right) \varphi_q \left(\zeta\right). \tag{2}$$

Here $\vec{\eta}^0$ is a unit vector directed along the positive η axis, and the functions $\varphi_q \left(\zeta\right)$ are defined as

$$\varphi_q \left(\zeta\right) = \begin{cases} \sin \alpha_{1q} \zeta, & 0 \leq \zeta \leq l_1; \\ A_q \sin \alpha_{2q} \zeta + B_q \cos \alpha_{2q} \zeta, & l_1 \leq \zeta \leq l_1 + l_2; \\ C_q \sin \alpha_{3q} \left(L - \zeta\right), & l_1 + l_2 \leq \zeta \leq L. \end{cases} \tag{3}$$

The subscript q is a serial number of the dispersion equation root for the LE_{q0}-mode, and α_{jq} $(j = 1, 2, 3)$ are transverse wave numbers. The expressions for A_q, B_q, C_q and α_{jq} are presented in Appendix A.

The unknown voltage amplitudes V_{qi} in Equation (1) can be found using the continuity condition of the tangential component of magnetic field H_ς on the surfaces S_1 and S_2 (Fig. 1(b)) as

$$H_\varsigma^0 + H_\varsigma^i \left(\vec{e}_{s1}\right) = H_\varsigma^v \left(\xi = 0\right), \quad \text{on } S_1 \tag{4}$$

$$H_\varsigma^v \left(\xi = t\right) = H_\varsigma^e \left(\vec{e}_{s2}\right), \quad \text{on } S_2. \tag{5}$$

The superscripts i and e designate the waveguide portions before and behind the diaphragm. The superscript v defines the area within the slot cavity, and H_ς^0 is an exciting field in the semi-infinite waveguide undisturbed by the slot.

The fields $H_\varsigma^i \left(\vec{e}_{s1}\right)$ and $H_\varsigma^e \left(\vec{e}_{s2}\right)$ can be easily found, since the magnetic dyadic Green's functions $\hat{G}^m \left(\vec{r}/\vec{r'}\right)$ for the semi-infinite regions i and e are known [13, 22–24]. The component $G_{11}^m \left(\vec{r}/\vec{r'}\right)$ in the form used in our paper is presented in Appendix B. Let us find the fields $H_\varsigma^v \left(\xi = 0\right)$ and $H_\varsigma^v \left(\xi = t\right)$ in the region "v". The electromagnetic field in this region can be presented as the fields of LE_{q0} modes propagating in the two opposite directions of ξ axis with amplitudes $V_q^\pm$. The superscript $\pm$ denotes the wave propagation directions: the sign plus if $\xi > 0$ and the sign minus if $\xi < 0$. The components of the electric $E_{\eta q}$ and magnetic $H_{\zeta q}$ field vectors of the LE_{q0} wave at arbitrary point ξ between the surfaces S_1 $(\xi = 0)$ and S_2 $(\xi = t)$ can be written as

$$E_{\eta q}^v \left(\xi\right) = \left[V_q^+ \exp\left(-i h_q \xi\right) + V_q^- \exp\left(i h_q \xi\right)\right] \varphi_q \left(\zeta\right)/d. \tag{6}$$

$$H_{\zeta q}^v \left(\xi\right) = \left[V_q^+ \exp\left(-i h_q \xi\right) - V_q^- \exp\left(i h_q \xi\right)\right] \varphi_q \left(\zeta\right) h_q/(dk W_0). \tag{7}$$

Here $k = 2\pi/\lambda$, h_q is the longitudinal wave number of the wave LE_{q0}. In the SI system of units $W_0 = 120\pi$. Using the representation in Equation (1) of the electric field on the surfaces S_1, S_2 and the expression (6) at $\xi = 0$ and $\xi = t$, we can find the relationship between the coefficients V_q^+, V_q^- and V_{q1}, V_{q2} as

$$V_q^+ = -[V_{q2} - V_{q1}\exp(ih_q t)]/(2i\sin h_q t), \tag{8}$$

$$V_q^- = [V_{q2} - V_{q1}\exp(-ih_q t)]/(2i\sinh_q t). \tag{9}$$

Substituting Equations (8) and (9) into Equation (7), we obtain the formula for the component $\vec{H}_{\zeta q}^v(\xi)$ of the magnetic field vector for the LE_{q0} wave at the arbitrary point ξ as

$$\begin{aligned}
H_{\zeta q}^v(\xi) = -\{&[V_{q2} - V_{q1}\exp(ih_q t)]\exp(-ih_q\xi) \\
&+ [V_{q2} - V_{q1}\exp(-ih_q t)]\exp(ih_q\xi)\}\varphi_q(\zeta)h_q/(2i\sin(h_q t)\,dkW_0).
\end{aligned} \tag{10}$$

The expression for the magnetic field component on the surfaces S_1 and S_2 can be obtained substituting $\xi = 0$ and $\xi = t$ intoformula (10).

$$H_{\zeta q}^v(0) = V_{q1}\frac{h_q}{i\tan(h_q t)\,dkW_0}\varphi_q(\zeta) - V_{q2}\frac{h_q}{i\sin(h_q t)\,dkW_0}\varphi_q(\zeta). \tag{11}$$

$$H_{\zeta q}^v(t) = V_{q1}\frac{h_q}{i\sin(h_q t)\,dkW_0}\varphi_q(\zeta) - V_{q2}\frac{h_q}{i\tan(h_q t)\,dkW_0}\varphi_q(\zeta). \tag{12}$$

Let us denote

$$R_{tq} = h_q/(iW_0kd\tan(h_q t)); \tag{13}$$

$$R_{sq} = h_q/(iW_0kd\sin(h_q t)). \tag{14}$$

Then, the component H_ζ^v of the magnetic field vector on the surfaces of the slot cavity $\xi = 0$ and $\xi = t$ can be written as

$$H_\zeta^v(\zeta, \xi = 0) = \sum_{q=1}^{Q}[V_{q1}R_{tq}\varphi_q(\zeta) - V_{q2}R_{sq}\varphi_q(\zeta)], \tag{15}$$

$$H_\zeta^v(\zeta, \xi = t) = \sum_{q=1}^{Q}[V_{q1}R_{sq}\varphi_q(\zeta) - V_{q2}R_{tq}\varphi_q(\zeta)]. \tag{16}$$

These equations allow us to reduce the functional Equations (4), (5) to the SLAE relative to the unknown amplitudes V_{q1} and V_{q2} using the Galerkin method as

$$\begin{cases}
\displaystyle\sum_{q=1}^{Q}V_{q1}(Y_{11,pq}^i + Y_{11,pq}^v) + \sum_{q=1}^{Q}V_{q2}Y_{12,pq}^v = F_p, \\[4mm]
\displaystyle\sum_{q=1}^{Q}V_{q1}Y_{21,pq}^v + \sum_{q=1}^{Q}V_{q2}(Y_{22,pq}^e + Y_{22,pq}^v) = 0.
\end{cases} \quad,\quad p = 1, 2, 3, \ldots, Q \tag{17}$$

Here

$$Y_{11,pq}^i = (-1)\int_{S_1}\left[\vec{e}_p^*, H_\zeta^i(\vec{e}_q)\,\vec{\zeta}^0\right]\vec{\xi}^0 dS; \tag{18}$$

$$Y_{22,pq}^e = \int_{S_2}\left[\vec{e}_p^*, H_\zeta^e(\vec{e}_q)\,\vec{\zeta}^0\right]\vec{\xi}^0 dS; \tag{19}$$

$$F_p = \int_{S_1}\left[\vec{e}_p^*, H_\zeta^0\vec{\zeta}^0\right]\vec{\xi}^0 dS. \tag{20}$$

The expressions $\left[\vec{e}_p^*, H_\zeta^{i(e)}(\vec{e}_q)\,\vec{\zeta}^0\right]\vec{\xi}^0$ in (18), (19) should be understood as $\vec{e}_p^* \times \vec{\zeta}^0 \cdot \vec{\xi}^0 H_\zeta^{i(e,0)}(\vec{e}_q)$, in Equation (20) and similarly in subsequent formulas.

Since $S_2 = S_1$,

$$Y_{11,pq}^v = Y_{22,pq}^v = R_{tq} \int_{S_1} \varphi_q(\zeta) \left[\vec{e}_p^*, \vec{\zeta}^0\right]\vec{\xi}^0 dS \tag{21}$$

and

$$Y_{12,pq}^v = Y_{21,pq}^v = (-1)\,R_{sq} \int_{S_1} \varphi_q(\zeta) \left[\vec{e}_p^*, \vec{\zeta}^0\right]\vec{\xi}^0 dS. \tag{22}$$

The fields $H_\zeta^i(\vec{e}_{s1})$ and $H_\zeta^e(\vec{e}_{s2})$ can be obtained using the Green's function for a semi-infinite waveguide. The integrands in Equations (21) and (22) have been obtained using equalities in Equations (15) and (16). The reflection and transmission coefficients S_{11} and S_{12} for the diaphragm considered can be found according the theory elaborated in [25, 26] (the main concepts of this theory are reviewed in [27]).

$$S_{11} = -1 + A_1, \quad S_{12} = B_1, \tag{23}$$

where

$$A_1 = -\frac{2}{N_1}\sum_{q=1}^{Q} V_{q1} \int_{S_1}\left[\vec{e}_q, \vec{H}^{(-1)}\right]\vec{n}\,dS,\ B_1 = -\frac{2}{N_1}\sum_{q=1}^{Q} V_{q2} \int_{S_2}\left[\vec{e}_q, \vec{H}^{(+1)}\right]\vec{n}\,dS,\ \text{and } N_1 = abkW_0\kappa_{10}^2\gamma_{10},$$

$\kappa_{10} = \pi/a$, $\gamma_{10} = \sqrt{k^2 - \kappa_{10}^2}$, $\vec{H}^{(\pm 1)}$ is a magnetic field vector of the H_{10}-mode, propagating in $z > 0$ (sign $+$) and $z < 0$ (sign $-$) directions (see Fig. 1), and $\vec{n}$ is a unit outward normal to the surface of the slot. The amplitude coefficients V_{qi} $(i = 1, 2)$ are to be found from the SLAE in Equation (17).

3. NUMERICAL SIMULATIONS AND EXPERIMENTAL RESULTS

The numerical simulations and experimental measurements were performed for the configuration similar to that shown in Fig. 1(b). The cross section ratios of two identical semi-infinite waveguides were $b/a = 0.435$. The slot was cut in the middle of the diaphragm which was of thickness t. The slot was of length L and of width d. The dielectric insert with length l and relative permittivity $\varepsilon_r > 1$ was placed in two positions: at the slot center and at the slot edge. The parameters of the insert corresponding to the configuration of Fig. 1(b) should be: $\varepsilon_1 = \varepsilon_3 = 1$ and $\varepsilon_2 = \varepsilon_r$, $l_2 = l$, $l_1 = l_3 = 0.5(L - l)$ when the insert is at the slot center and $l_2 = l$, $l_1 = L - l$, $l_3 = 0$ when the insert is at the slot end. Modules of the reflection $|S_{11}|$ and transmission $|S_{12}|$ coefficients were calculated in waveband of the single-mode waveguide using the relations in Equation (23).

The frequency or wavelength at which the minimum of reflection coefficient $|S_{11}|$ is observed will be called the slot resonant frequency f_{res} or resonant wavelength λ_{res}. Simulation results are shown in Figs. 2–5. The convergence of results was evaluated by finding the number of approximating basis functions Q required for the stabilization of the estimated resonant wavelength λ_{res}. The resonant wavelength obtained with Q basis functions is denoted as $\lambda_{res,Q}$.

Figures 2(a) and 2(b) present the frequency dependency of the reflection coefficient $|S_{11}|$ obtained near $\lambda_{res,Q}$, for the two positions of the dielectric insert and various Q ($Q = 1$, 3, 5, 7, 11 15). The curves for $Q = 19$, and $Q = 23$ which were calculated, are not shown in Fig. 2 because $\lambda_{res,23}$ and $\lambda_{res,19}$ differ from $\lambda_{res,15}$ not more than by 0.1%. So, three of them are practically not distinguishable, and we may assume that $\lambda_{res,15} \cong \lambda_{res}$. Let $\Delta\lambda_Q = \lambda_{res} - \lambda_{res,Q}$, then Fig. 2 shows that the approach with $Q = 1$ is better when the dielectric insert is located at the slot center ($\Delta\lambda_1/\lambda_{res} < 2\%$) than when the insert is near the slot end ($\Delta\lambda_1/\lambda_{res} \approx 5\%$). It can also be seen that $\Delta\lambda_7/\lambda_{res} \leq 0.2\%$ when $Q = 7$ and $\Delta\lambda_{11}/\lambda_{res} \leq 0.1\%$ when $Q = 11$. The further calculations were carried out at $Q = 11$.

In order to obtain the same resonant wavelengths for the edge and central positions of the insert, it must be three times longer at the edge position than when it is centered.

Dependence of the resonance wavelength on the permittivity ε_r for the two positions of the layer is shown in Fig. 3. The resonance wavelength strongly depends on the permittivity and the length of the insertion plate when it is placed in the center of the slot.
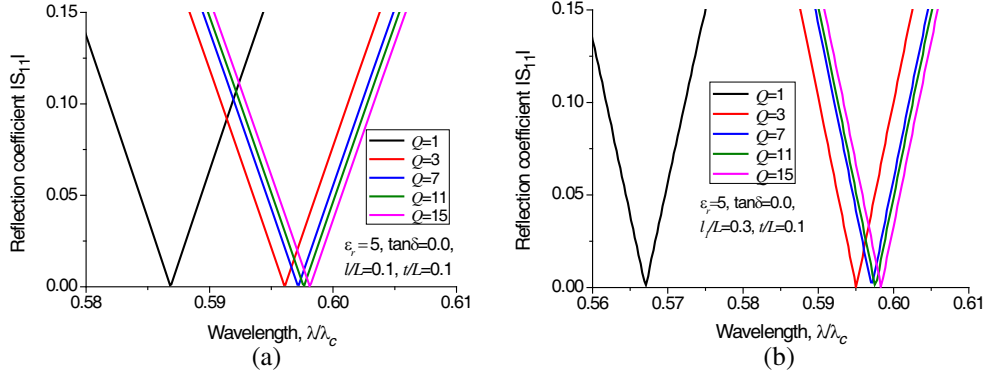
Figure 2. The reflection coefficient $|S_{11}|$ versus normalized wavelength λ/λ_c, $a \times b = 23 \times 10\,\mathrm{mm}^2$, $L = 12\,\mathrm{mm}$, $d = 1.2\,\mathrm{mm}$, $\varepsilon_r = 5$, (a) the dielectric insert at the slot center, (b) the dielectric insert at the slot edge.
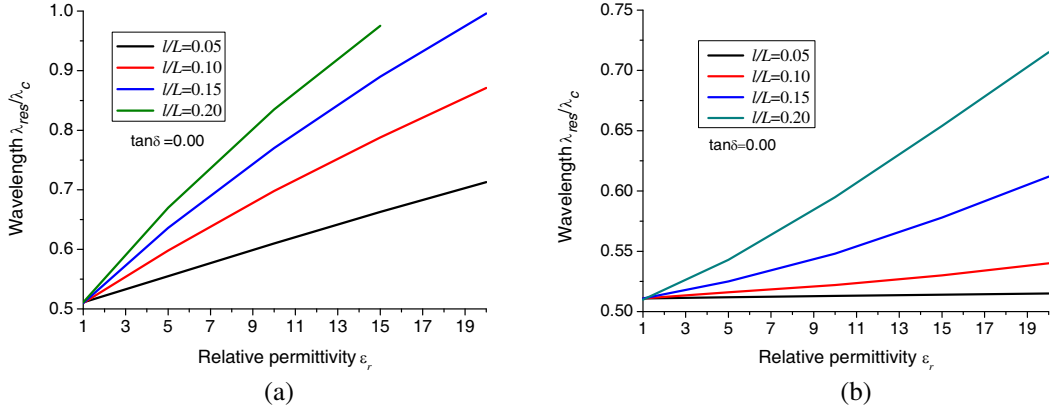
Figure 3. The resonant wavelength of the slot versus the insert permittivity, $a \times b = 23 \times 10\,\mathrm{mm}^2$, $L = 12\,\mathrm{mm}$, $d = 1.2\,\mathrm{mm}$, (a) the dielectric insert in the slot center, (b) the dielectric insert at the slot edge.

Comparing the plots in Fig. 3(a) and Fig. 3(b), one can see that the position of the dielectric insert has a significant influence on the slot resonant wavelength. For example, when $l/L = 0.1$ and $\varepsilon_r = 10$, the slot resonant wavelength is almost 34% higher for the central insert position compared to its position at the slot edge. This effect can be used for slot resonant tuning by varying the insert position in the slot.

Let us now consider the reflection and transmission coefficients $|S_{11}|$ and $|S_{12}|$ when the insert is made of perfect or non-perfect dielectric, $\tan\delta = 0$ or $\tan\delta > 0$. The wavelength dependence of $|S_{11}|$ and $|S_{12}|$ plotted for the insert with $\varepsilon_r = 10(1 - i\tan\delta)$ and for various $\tan\delta$ are shown in Fig. 4. As can be seen, the slot resonant frequency weakly depends upon the dielectric losses.

As can be seen from Fig. 4, the minimum of the reflection coefficient is $|S_{11}| = 0$ for the perfect dielectric insert, therefore VSWR $= 1$, and $|S_{12}| = 1$. Thus, the incident power completely penetrates through the slot into the waveguide behind the diaphragm. When the dielectric insert is lossy ($\tan\delta > 0$), at the resonance inequalities VSWR > 1, $|S_{11}| > 0$ take place. This causes the maximum of the transmission coefficient $|S_{12}|$ to decrease (Fig. 4), so that inequality $|S_{11}|^2 + |S_{12}|^2 < 1$ is fulfilled, i.e., a part of the power is consumed for dielectric's heating.

Let us now evaluate what part of the incident power is consumed for dielectric heating and introduce the power absorption coefficient $|S_\sigma|^2$, which can be defined from the power balance equation as

$$|S_\sigma|^2 = 1 - \left(|S_{11}|^2 + |S_{12}|^2\right).$$
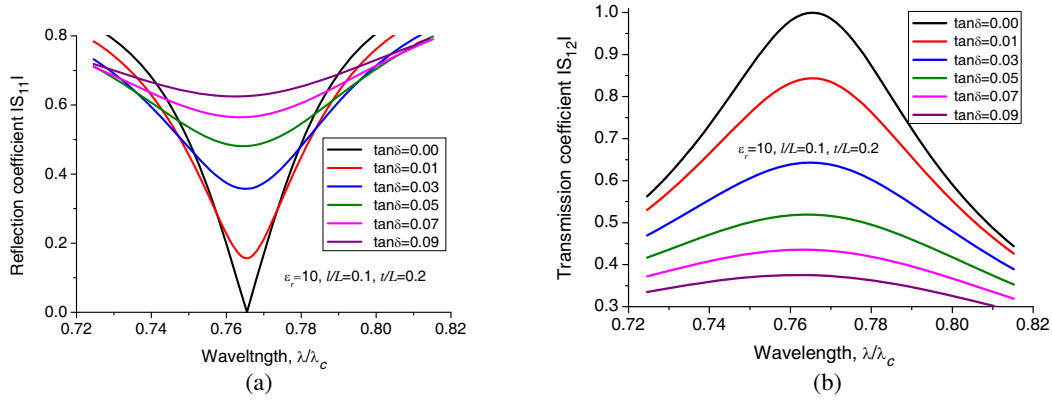
Figure 4. Wavelength dependence of the reflection $|S_{11}|$ and transmission $|S_{12}|$ coefficients for various losses, $a \times b = 23 \times 10\,\text{mm}^2$, $L = 12\,\text{mm}$, $d = 1.2\,\text{mm}$, (a) reflection coefficients, (b) transmission coefficients.
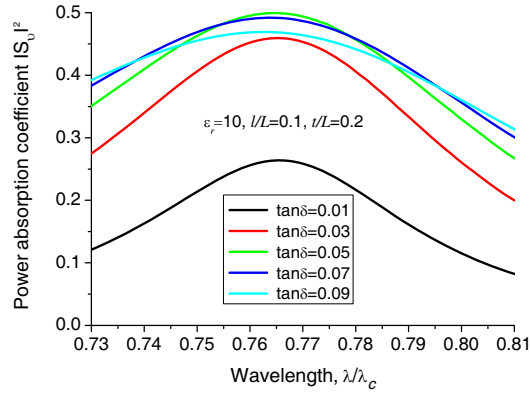
Figure 5. The power absorption coefficient $|S_\sigma|^2$ versus the wavelength, $a \times b = 23 \times 10\,\text{mm}^2$, $L = 12\,\text{mm}$, $d = 1.2\,\text{mm}$.

The wavelength plots of the power absorption coefficient $|S_\sigma|^2$ for various $\tan\delta$ are shown in Fig. 5. It can be seen that the coefficient $|S_\sigma|^2$ increases with increasing losses till the reflection and transmission coefficients, $|S_{11}|$ and $|S_{12}|$, become equal to 0.5 (Fig. 4). The power absorption coefficient increases from zero when $\tan\delta = 0$ to a maximum equal to 0.5, when $\tan\delta = 0.05$ in the case shown in Fig. 5. As $\tan\delta$ the further increases the resonant value of coefficient $|S_\sigma|^2$ begins to decrease. An analogous effect can be observed for a slot radiating from an infinite waveguide into free half-space: a resonant slot can radiate no more than a half of the power, propagating from a generator [25, 26]. Thus, the coefficient $|S_\sigma|^2$ defining the power spent for dielectric heating is, in certain aspect, similar to the radiation coefficient $|S_\Sigma|^2$ of the slot radiating into the free-space or some other infinite electro-dynamical volume.

The numeric simulations have also revealed that the resonant wavelength λ_{res} of the slot increases if the diaphragm thickness is increased, and approaches the critical wavelength of the waveguide, equivalent to the slot with a dielectric. It was also observed that when $l/L \leq 0.1$, $\varepsilon_r \leq 10$ and $t/L \leq 0.1$, the losses defined by $\tan\delta \leq 0.1$ do not vary the resonant wavelength of the slot. With an increase in losses when $\tan\delta \geq 0.1$ during the same geometry a slow decrease in the resonant frequency is observed. For example at $l/L \leq 0.1$, $\varepsilon_r = 10$, $t/L = 0.2$ and $\tan\delta = 0.4$ resonance frequency is shifted by 1.1% compared to an ideal dielectric.

Correctness of the model was validated by VSWR measurements for the configuration shown in Fig. 1 (the waveguide cross section $a \times b = 28.5 \times 12.6\,\text{mm}^2$) for two positions of the insert: at the slot center and at its edge. The measurements were carried out on the panoramic VSWR-meter P2-60 with accuracy not less than 0.2%. The VSWR of the termination load was not higher than 1.06. The insert

was made of the material PTFE-4 with permittivity in the range $1.92 \leq \varepsilon_r \leq 2.2$ and $\tan \delta = 0.0002$ at $f = 10$ GHz. Dielectric PTFE-4, which was produced in the USSR, is an analogue of Teflon (made in the USA).

The VSWRs as function of the frequency plotted using the simulation and experimental data are shown in Fig. 6 for the two insert positions. The parameters of the dielectric insert are given in the plots. The simulation data were obtained for ε_r equal to 2.0, 1.98, 1.96, and 1.94 that belong to the range of possible variation of the PTFE-4 permittivity $1.92 \leq \varepsilon_r \leq 2.2$.
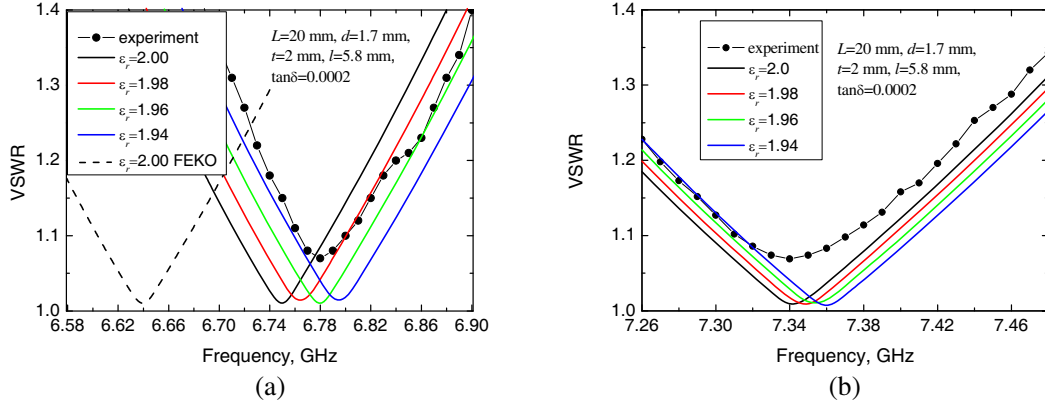
Figure 6. The simulated and experimental VSWR versus the frequency ($a \times b = 28.5 \times 12.6 \, \text{mm}^2$): (a) the dielectric insert at the slot center, (b) the dielectric insert at the slot edge.

The analysis of the plots shows that the slot resonant frequency for the four values of permittivity varies in ranges from 6.8 to 6.75 GHz when the insert is at slot center. When the insert is at the slot edge, the resonant frequency varies in the range from 7.36 to 7.34 GHz. In the latter case, the frequency variation is about 0.3%, which is comparable with the accuracy of frequency measurement. The measured resonant frequencies for both slot positions are in the ranges predicted by the model, and thus confirm its validity. The simulation results show that the slot resonant frequency for the central slot position is more sensitive to changes of the insert permittivity ε_r than for the edge slot position. When the insert is located at the slot edge, small differences between the permittivity of the real insert material and that used in simulation, for example $\varepsilon_r = 2$, causes practically undistinguishable resonant frequencies f_{res} (Fig. 6(b)), as compared to that for the central slot position (Fig. 6(a)).

The simulation results shown in Fig. 3 combined with experimental data allow us to estimate permittivity of the insert made of an unknown material. It can be done in the following way. Suppose that we have calculated resonance wavelength depending on ε_r for the system considered. After this, we experimentally determine the resonant wavelength for this system. Using the numerically obtained dependency λ_{res}/λ_c versus ε_r like those shown in Figs. 3(a) or 3(b), one can estimate the corresponding value of ε_r. The level of $|S_{11}|$ minimum at the resonance frequency shows us, according to Fig. 4, if losses in the dielectric slab are present or not.

In Fig. 6(a), the dashed line corresponds to data obtained by numerical method (simulator FEKO) for $\varepsilon_r = 2$. The resonance frequency on this curve ($f_{res} = 6.64$ GHz) differs by 1.6% from one ($f_{res} = 6.75$ GHz), obtained in our calculations, and by 2% from experimental value ($f_{r,\exp} = 6.78$ GHz). The reason for these minor discrepancies may be the following. The simulator FEKO, as we think, automatically takes into account the electrical field singularity on the mathematically sharp slot edge. Unlike the papers in [28–30], we did not supply the basic functions in Equation (2) with the factor accounting the $\vec{E}$ field singularity at the edges of the slot. Using 11 basic functions in Equation (1), we obtained a good converged value for f_{res}. It was astonishing that our numerical results matched with the experiment much better than those obtained by using simulation FEKO. Perhaps the reason is that we cannot reach the mathematical sharpness of edges in experimental samples. Let $\Delta f = |f_{r,\exp} - f_{res}|$. It happened so that, according to Fig. 6(a), for all ε_r from the interval $1.92 \leq \varepsilon_r \leq 2.2$, the value of $\Delta f / f_{r,\exp}$ does not exceed the level of 0.045% which is less than a possible error of a frequency measurement by the panoramic VSWR-meter P2-60.

The reason for the differences in the experimental and calculated minima values of the VSWR in the frequency dependence is as the following. In our case, the estimated values of VSWR at the minimum for dielectric with low losses is equal to 1.011. Panoramic VSWR-meter does not allow to measure the VSWR at a level below 1.06. Therefore, the difference inevitably exists between the calculated and experimental minimal values of VSWR in Fig. 6.

4. CONCLUSION

The problem of dominant wave scattering by a slotted diaphragm in the rectangular waveguide has been solved. The narrow slot cut in the diaphragm is partially filled with a dielectric insert. The mathematical model of this structure is based on the idea of the field representation in the slot cavity as a set of eigenwaves in a waveguide equivalent to the slot. The simulation results were obtained using 1, 3, 7, 11 and 15 basis functions. The mathematical model ensures a good convergence of the results even if the slot electric field is approximated by a limited number of basis functions. The model validity was confirmed by the experimental results.

The simulation results were obtained for the inserts made of perfect and non-perfect dielectric. It was found that the losses in a thin dielectric insert with $\varepsilon_r \leq 10$ and $\tan\delta \leq 0.4$ did not shift the slot resonant frequency, but significantly increased the resonant reflection coefficient. The maximum heating of the non-perfect dielectric in the slot occurred when the resonant reflection coefficient of the slotted diaphragm was 0.5. A comparative analysis of simulated and experimental data allows estimating the insert permittivity and dielectric losses. The dielectric insert in the slot can be used as an additional control element to vary the wavelength of the resonant slot. The results obtained in this paper can also be used for the effective irradiation and heating of small dielectric samples and for studying their electrical properties.

APPENDIX A.

$$A_q = \frac{\alpha_{1q}}{\alpha_{2q}} \cos\alpha_{1q}l_1 \cos\alpha_{2q}l_1 + \sin\alpha_{1q}l_1 \sin\alpha_{2q}l_1;$$

$$B_q = \sin\alpha_{1q}l_1 \cos\alpha_{2q}l_1 - \frac{\alpha_{1q}}{\alpha_{2q}} \sin\alpha_{2q}l_1 \cos\alpha_{1q}l_1;$$

$$C_q = \frac{\dfrac{\alpha_{1q}}{\alpha_{2q}} \sin\alpha_{2q}l_1 \cos\alpha_{1q}l_1 + \sin\alpha_{1q}l_1 \cos\alpha_{2q}l_1}{\sin\alpha_{3q}l_3}.$$

$\alpha_{jq} = \sqrt{k^2\varepsilon_{rj} - h_q^2}$, where h_q is a root of the dispersion equation for LE_{q0}-mode.

APPENDIX B.

$$G_{11}^m\left(\vec{r}/\vec{r}'\right) = \frac{4\pi}{ab} \sum_{m,n} \frac{\varepsilon_m\varepsilon_n}{i\gamma_{mn}} \sin\frac{m\pi x}{a} \sin\frac{m\pi x'}{a} \cos\frac{n\pi y}{b} \cos\frac{n\pi y'}{b} \cos\gamma_{mn}z' e^{-i\gamma_{mn}z}.$$

Here $\varepsilon_m = (2 - \delta_{om})$, $\varepsilon_n = (2 - \delta_{on})$, the symbols δ_{om}, δ_{on} denote the Kronecker's delta; x, y, z and x', y', z' (primed) are coordinates of observation and source points;

$$\gamma_{mn} = \sqrt{k^2 - \left(\frac{m\pi}{a}\right)^2 - \left(\frac{n\pi}{b}\right)^2}$$

REFERENCES

1. Pocklington, H. C., "Electrical oscillations in wires," *Proc. Cambr. Phil. Soc.*, Vol. 9, No. 7, 324–332, 1897.

2. Hallen, E., "Theoretical investigation into transmitting and receiving antennas," *Nova Acta (Ups.)*, Ser. 4, Vol. 11, No. 1, 1–44, 1938.

3. Leontovich, M. A. and M. L. Levin, "Theory of oscillations in dipole antennas," *Journal of Technical Physics*, Vol. 14, No. 9, 481–506, 1944.

4. Watson, W. H., "Resonant slots," *Journal of IEEE*, Part A, Vol. 93, 747–777, 1946.

5. Feld, Y. N., *Fundamentals of the Theory of Slot Antennas*, Sov. Radio, Moskow, 1948 (in Russian).

6. Stevenson, A. F., "Theory of slots in rectangular waveguides," *Journal of Applied Physics*, Vol. 19, 24–38, 1948.

7. Dmitriev, V. I. and E. V. Zakharov, "Numerical solution of some Fredholm integral equations of the first kind," *Computational Methods and Programming*, Vol. 20, 49–54, Moskow State Univers., 1968 (in Russian).

8. Lerer, A. M. and A. G. Schuchinsky, "Full-wave analysis of three-dimensional planar structures," *IEEE Transactions on Microwave Theory and Techniques*, Vol. 41, 2002–2015, 1993.

9. Lerer, A., I. Donets, and S. Bryzgalo, "The semi-inversion method for cylindrical microwave structures," *Journal of Electromagnetic Waves and Applications*, Vol. 10, No. 6, 765–790, 1996.

10. Eminov S. I., "Theory of integral equation of thin dipole," *Technology and Electronics*, Vol. 38, No. 12, 2160–2168, 1993 (in Russian).

11. Plotnikov, V. N., Y. Y. Radtsig, and S. I. Eminov, "Theory of integral equation of narrow rectangular slot," *Computational Mathematics and Mathematical Physics*, Vol. 34, No. 1, 68–77, 1994 (in Russian).

12. Kravchenko, V. F., O. S. Labunko, A. M. Lerer, and G. P. Sinyavsky, *Computing Methods in the Modern Radiophysics*, Fizmatlit, Moskow, 2009 (in Russian).

13. Nesterenko, M. V., V. A. Katrich, Y. M. Penkin, and S. L. Berdnik, "Analytical methods in theory of slot-hole coupling of electrodynamics volumes," *Progress In Electromagnetics Research B*, Vol. 70, 80–174, 2007.

14. Garb, H. L., I. B. Levinson, and P. S. Fredberg, "Effect of wall thickness in slot problems of electrodynamics," *Radio Eng. Electron. Phys.*, Vol. 13, 1888–1896, 1968.

15. Panchenko, B. A., "Electromagnetic wave diffraction by a plane screen of finite thickness with regularly placed openings," *Technology and Electronics*, Vol. 12, 719–722, 1967.

16. Khac, T. V. and C. T. Carson, "Coupling by slots in rectangular waveguides with arbitrary wall thickness," *Electronics Letters*, Vol. 8, 456–458, 1972.

17. Yatsuk, L. P. and V. A. Katrich, "Slot coupling elements with partially dielectric filling," *Izv. Vuzov. Radioelectronics*, Vol. 22, No. 2, 60–65, 1979 (in Russian).

18. Klimenko, V. A., "Resonance diaphragm of finite thickness partially filled with dielectric in a rectangular waveguide," *Technology and Electronics*, No. 3, 499–507, 1980 (in Russian).

19. Jia, H., K. Yoshitomi, and K. Yasumoto, "Rigorous and fast convergent analysis of a rectangular waveguide coupler slotted in common wall," *Progress In Electromagnetics Research B*, Vol. 46, 245–264, 2004.

20. Katrich, V. A., M. V. Nesterenko, and N. A. Khiznyak, "Asymptotic solution of integral equation for magnetic current in slot radiators and coupling apertures," *Telecommunication and Radio engineering*, Vol. 63, 89–107, 2005.

21. Yatsuk, L. P., A. V. Podcheko, and V. V. Reimer, "Waveguides wave scattering by narrow slots with stratified dielectric," *URSI Proc. International Symposium on Electromagnetic Theory*, 39–41, St. Petersburg, 1995.

22. Morse Ph. M. and H. Feshbach, *Methods of Theoretical Physics*, Part II, New York Toronto London McGraw Hill Book Company, Inc. 1953.

23. Markov, G. T. and B. A. Panchenko, "Tensor Green's functions of rectangular waveguides and resonators," *Izv. VUZ'ov. Radiotekhnika*, Vol. 7, No. 1, 34–41, 1964.

24. Panchenko, B. A., "Tensor Green's functions of Maxwell equations for the cylindrical domains," *Radiotekhnika: Coll. Sci. Proceedings*, No. 15, 82–91, Kharkov, 1970 (in Russian).

25. Feld, Y. N. and L. S. Benenson, *Antenna-Fider Devices*, N. E. Zhukovsky Air Forces Academy, Moscow, 1959 (in Russian).

26. Feld, Y. N. and L. S. Benenson, *Fundamentals of Antenna Theory, Textbook for High Schools*, Drofa, Moskow, 2007 (in Russian).

27. Yatsuk, L. P., "Development of the Fel'd's concepts on the slotted waveguide devices in the works of researchers from the Karazin National University," *Journal of Communications Technology and Electronics*, Vol. 57, 964–971, 2012, ISSN 106412269.

28. Schuchinsky, A. G., D. E. Zelenchuk, A. M. Lerer, and R. Dickie, "Full-wave analysis of layered aperture arrays," *IEEE Transactions on Antennas and Propagations*, Vol. 54, 490–502, 2006.

29. Zemlyakov, V. V., G. F. Zargano, and S. V. Krutiev, "Waveguide bandpass filter on complex resonance diaphragms," *Journal of Communications Technology and Electronics*, Vol. 60, 1305–1310, 2015.

30. Zemlyakov, V. V. and G. F Zargano, "Electrodynamic analysis of conductivity of a resonance waveguide plane-transverse diaphragm with a complex aperture," *Radiophysics and Quantum Electronics*, Vol. 58, 504–510, 2015.